RASĀYAN *J. Chem.*
Vol. 19 | No. 2 | 1069-1078| April-June | 2026
ISSN: 0974-1496 | e-ISSN: 0976-0083 | CODEN: RJCABP
http://www.rasayanjournal.com
http://www.rasayanjournal.co.in

SYNTHESIS AND CHARACTERIZATION OF NiS/ZrS_2 NANOPARTICLES BY ELECTROCHEMICAL METHOD: PHOTODEGRADATION KINETICS OF METHYLENE BLUE DYE AND INVESTIGATION OF ITS ANTIBACTERIAL ACTIVITIES

H. S. Sindhushree[1], R.T. Radhika[2], and B. M. Venkatesha[1,✉]
[1]Department of Chemistry, Yuvaraja's College, University of Mysore, Mysuru, India
[2]Department of Chemistry, Government first Grade College, Kuvempunagara, Mysuru, India
✉Corresponding author: bmvenkatesha123@gmail.com

ABSTRACT

This study reports the synthesis and characterization of novel NiS/ZrS_2 nanocomposite particles via a facile electrochemical method and evaluates their photocatalytic and antibacterial potential. Zirconium sulphide (ZrS_2), with a direct band gap of 2.48 eV, is a promising semiconductor for optical applications. The electrochemical synthesis produced NiS/ ZrS_2nanoparticles, whose structural, morphological, compositional, and optical properties were investigated using X-ray diffraction (XRD), Fourier Transform Infrared (FTIR) spectroscopy, Field Emission Scanning Electron Microscopy with Energy Dispersive X-ray spectroscopy (FESEM/EDAX), and UV-Visible (UV-Vis) spectroscopy. XRD analysis confirmed the crystalline nature of the composite, while FESEM revealed its surface morphology and EDAX verified elemental composition. Optical studies utilizing UV-Vis spectroscopy were employed to determine the band gap energy, and FTIR identified functional groups. The photocatalytic performance of the synthesized nanoparticles was assessed by studying the degradation kinetics of Methylene Blue (MB) dye under light irradiation. The results demonstrated efficient photodegradation, highlighting the material's potential for environmental remediation of organic pollutants. Furthermore, the NiS/ ZrS_2nanoparticles exhibited significant antibacterial activity against both Gram-positive and Gram-negative bacteria, specifically *Bacillus subtilis*, *Lactobacillus acidophilus*, and *Staphylococcus aureus*. This work presents a straightforward synthesis route for a multifunctional NiS/ ZrS_2nanocomposite with promising applications in photocatalysis and biomedical fields.

Keywords: NiS/ZrS_2 Nanoparticles, Methylene Blue Dye, Electrochemical Method, Antibacterial Activity, Photocatalysis

RASĀYAN*J. Chem.*, Vol. 19, No. 2, 2026

INTRODUCTION

A lot of attention has recently been paid to semiconductor nanocrystals because of their special optical and physicochemical characteristics.[1] The applications for metal sulphide nanoparticles are numerous, ranging from cosmetics to therapeutics and diagnostics. They exhibit enhanced electrical and structural integrity, improved magnetic properties, and increased optical activity. The excellent chemical and physical properties of the nanoparticles vary according to their size.[2] The last twenty years have seen a rapid advancement in the different methods used to fabricate nanoparticles.[3-4] Because of the layered structures that result from van der Waals interactions, sulfide metal is widely used. Because of sulphur's high polarizability, low melting point, and volatilization, nonstoichiometric material is produced. Comparing the Ni-S system to other transition metal sulphides, the phase diagram is more complicated. Because of their low cost, high electrical conductivity, large theoretical capacitance, and environmentally favorable qualities, extensive research has focused on metal sulphides.[5-8] NiS is a crucial component of an inorganic transition metal that, either through doping or temperature-dependent, exhibits a metal-insulator transition.[9]

The measured properties of ZrS_2 include a band gap of 1.68 eV and a stoichiometry approximating the ideal chalcogen-to-metal ratio of 2.[10-11] Because of its great corrosion resistance, zinc is a transition metal that is mostly used as an opacifier and refractory. It is also occasionally used as an alloying agent.

Although zirconium has no known biological function, compounds containing Zirconium are used in numerous biomedical applications, such as knee and hip replacements, dental implants, and other restorative procedures.[12-14] In this regard, NiS/ZrS_2nanocomposites were created using a novel electrochemical technique, and their catalytic effects on the antibacterial activity and photocatalytic degradation of Methylene Blue dye were noted.

EXPERIMENTAL

Materials and Apparatus

The chemicals used for the study of electrochemical synthesis of NiS/ZrS_2 nanoparticles were of analytical grade purity. Sodium sulphide, Ni, and Zr wires were purchased from Alfa Aesar Pvt Ltd. All experiments were conducted using deionised water generated by a PURELAB Ultra purification system.

Electrochemical Synthesis of NiS/ZrS_2 Nanoparticles

The process used to synthesise the NiS/ZrS_2 nanoparticles is an electrochemical method. Figure-1 depicts the process of the experiment. The 20ml of 0.2M Na_2S solution is used to dip the two metal wires, Ni and Zr. The platinum electrode is connected to the positive terminal of the cathode, and the Ni and Zr metal wires to the Negative terminal of the battery. With constant stirring, the experiment was conducted for two hours using a potential of 10V and a current of 15 mA. During electrolysis, the anode and cathode were separated by 2 cm. The Ni and Zr wires begin to dissolve during the electrolysis process, releasing Ni and Zr ions. These ions then electrochemically react with Na_2S to produce sulfide along with Ni and Zr ions. The possible mechanism for the electrochemical synthesis of NiS/ZrS_2 is shown in Scheme-1. After obtaining the solid, it is thoroughly cleaned of any unreacted Na_2S using double-distilled water. To remove salt and hydroxide contaminants, the material is centrifuged and calcined for two hours at 750 °C.[15]

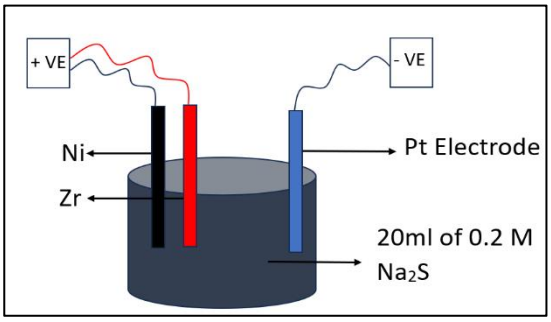

Fig.-1: Electrochemical SynthesisSetupfor NiS/ZrS_2 Nanoparticles

$$Ni \rightleftharpoons Ni^{2+} + 2e^-$$
$$Na_2S \rightleftharpoons 2Na^+ + S^{2-}$$
$$Ni^{2+} + S^{2-} \rightleftharpoons NiS$$
$$Zr \rightleftharpoons Zr^{4+} + 2e^-$$
$$2Na_2S \rightleftharpoons 2Na^+ + 2S^{2-}$$
$$Zr^{4+} + 2S^{2-} \rightleftharpoons ZrS_2$$
$$\text{The overall Reaction is } Ni \xrightarrow[Na_2S]{Zr} NiS/ZrS_2 \text{ Nano Composite}$$

Scheme-1: Electrochemical Synthesis Mechanism of NiS/ZrS_2 Nanoparticles

Evaluating Photocatalytic Activity

A 3×10^{-5} M Methylene Blue dye solution was prepared by dissolving it in distilled water. The prepared NiS/ZrS_2nanoparticles'photocatalytic activities were assessed using this solution as a test contaminant. The investigation was conducted in tungsten-halogen ultraviolet light to verify the efficiency of NiS/ZrS_2nanoparticles. A centrifuge tube was filled with 20 millilitres of dye solution in order to measure the photocatalytic activity. The catalyst was dispersed, and the dye solution percentage transmittance was

noted after centrifuging at 800 rpm. Reports of Chemical oxygen demand (COD) have been made using the dichromate oxidation method both prior to and following the deterioration of the Methylene Blue dye solution. COD values were obtained using the following expression.[16]

$$COD=\frac{(Blank-Sample)X\ NFAS\ X\ 8000}{Vsample}(1)$$

Analysis and implications

X-Ray Diffraction (XRD) Analysis

The X-ray diffraction (XRD) pattern for the synthesized NiS/ZrS_2 nanoparticles is presented in Fig.-2(a). The dominant diffraction peaks of NiS/ZrS_2 nanoparticles appear at 2 thetaand are confirmed by the XRD data. These peaks are 35.77, 40.54, and 48.93 planes of (021), (211), and (131) with reference to JCPDS card number 65-2117 for NiS.[17] The 2 theta in degrees of 30.14, 50.33, and 62.66 planes of (002), (110), and (004), respectively, with reference to JCPDS card number 03-1099 for ZrS_2.[18]Based on the Debye-Scherrer equation ($D = k\lambda/\beta\cos\theta$), analysis of the X-ray diffraction data presented in Fig.-2(b) indicates that the synthesized NiS/ ZrS_2nanoparticles possess an average crystallite size of approximately 2.27 nm and exhibit a hexagonal crystal structure. In the Debye-Scherrer equation, λ denotes the wavelength of the incident X-ray beam, **β** represents the full width at half maximum of the measured diffraction peak, θ is the corresponding Bragg angle, and **k** is a dimensionless shape factor, commonly taken as 0.9.19

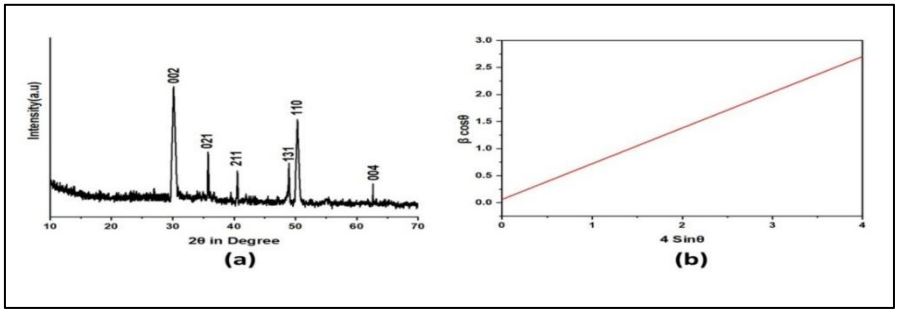

Fig.-2: NiS/ZrS_2 Nanoparticles (a) XRD Pattern, and (b)WH Plot

Ultra Violet-Visible Spectra

The optical absorption spectra of the NiS/ZrS_2 nanoparticles have confirmed that the observed blue shift in the absorption spectrum can be attributed to an increase in the band gap energy caused by the nanoscale particle size.[19] The synthesised NiS/ZrS_2 nanoparticles, as seen in Fig.-3, have a maximum intensity peak in the UV region at 420.23 nm shown in Fig.-3 (a). In addition, dye degradation occurs much more slowly in the presence of sunshine than it does in the ultraviolet. The synthesised nanoparticles are photoactive when exposed to ultraviolet light, as evidenced by the NiS/ZrS_2 nanoparticles' UV-visible spectrum, which spans 200–800 nm. Using the Tauc plot, the band gap of synthesised NiS/ZrS_2 nanoparticles was determined by plotting $(\alpha hm)^{½}$versus hγ. The synthesised NiS/ZrS_2 nanoparticles were found to have band gap energy of 2.48 eV shown in Fig.-3 (b).

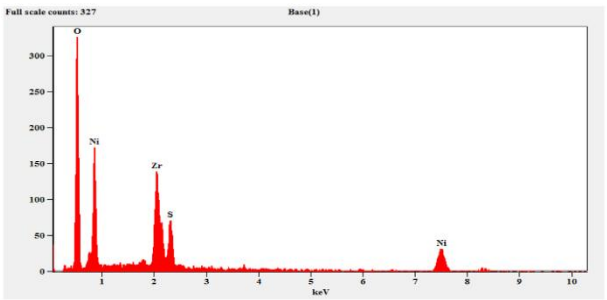

Element	Weight %	Atom %
O K	53.84	81.96
S K	5.17	3.93
Ni K	21.42	8.89
Zr L	19.57	5.23
Total	100.00	100.00

Fig.-3: NiS/ZrS_2 Nanoparticles (a) Ultra Violet-Visible Spectra, and (b) Tauc Plot

Scanning Electron Microscopy (SEM)

High-resolution microscopy, or SEM, provides detailed surface information about solid materials. It is evident from Fig.-4 that the particles were aggregated with Nisand Zr. When viewed at various magnifications, the SEM image reveals that the NiS/ZrS_2 nanoparticles have a spherical structure. The SEM image displays NiS that has been randomly distributed along with smaller-sized ZrS_2 grains seen in Fig.-4.

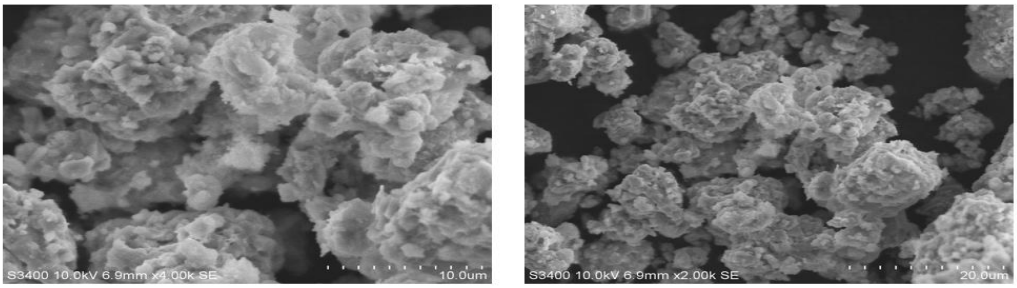

Fig.-4: NiS/ZrS_2 Nanoparticles SEM Images

EDAX

Ni, Zr, S, and O were confirmed to be present in the nanomaterial by the EDAX mapping. The values obtained indicate Ni percentage, which is higher compared with the Zr, and S was lower compared to all the elements shown in Fig.-5.

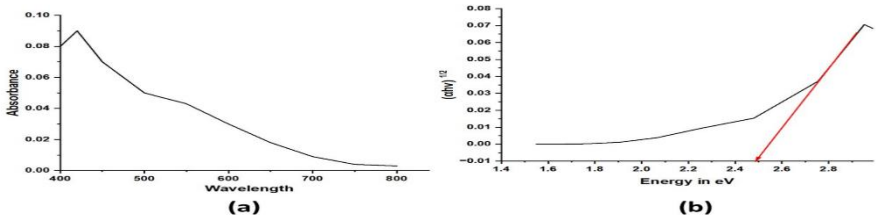

Fig.-5: NiS/ZrS_2Nanoparticles EDAX Mapping Graph

Fourier Transform Infrared Spectroscopy (FT-IR) Spectra

The functional groups present in the substance were identified by Fourier-transform infrared (FTIR) spectroscopy, as shown in Fig.-6. A Perkin Elmer spectrometer was employed to determine the modes of vibration of the chemical bonds in the NiS/ZrS_2 nanoparticles FT-IR spectra. These modes have been recorded between 500 and 4000 cm^{-1}. Chemically bound hydroxyl groups are indicated by the wide peak at 3241.90 cm^{-1}. The Metal-Oxygen is associated with the three peaks at roughly 1088.58, 1597.99, and 3271.90.[20]

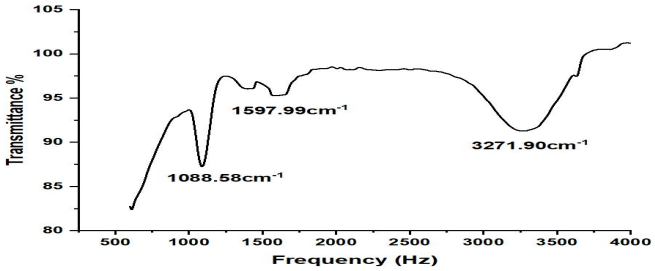

Fig.-6: NiS/ZrS_2 Nanoparticles FTIR Spectra

Degradation Kinetics and Chemical Oxygen Demand (COD) Analysis

Effect of Concentration of Methylene Blue Dye

Methylene blue (MB), commonly referred to as basic blue 9, was selected as the cationic dye mentioned in Table-1.[21]The effect of dye concentration was investigated using a series of four methylene blue

solutions with varying molarities ($1x10^{-5}$, $2x10^{-5}$, $3x10^{-5}$, and $4x10^{-5}$) with constant weight NiS/ZrS_2 nanoparticles serving as a catalyst. The colour change was measured using a spectrophotometer, and the log %T (percentage of light transmitted) against time plot revealed a linear trend of the reaction, demonstrating that Methylene Blue discolouration was present in Fig.-7(a). According to Table-2 rate constant values, the reaction rate falls as the Methylene Blue dye concentration raises. Increased dye concentration strongly colours the solution. This decreases the travel length of photons entering the solution, slowing their arrival at the catalyst surface. Consequently, there are fewer. Scheme-2 illustrates the production of ·OH hydroxyl free radicals and the possible photodegradation pathway mechanism of MB dye is shown in Scheme-3. Consequently, photodegradation efficiency is reduced.[22] The COD values for the Methylene Blue dye solution are displayed in Table-1, both prior to and following the degradation depicted in Fig.-7(b). The photocatalyst's photodegradation efficiency was calculated using the following formula (2).

$$\text{Photodegradation Effieciency} = \frac{\text{Starting COD-Ending COD}}{\text{Starting COD}} \qquad (2)$$

Table-1: Properties of Methylene Blue Dye

Dye	Chemical Formula	Molar Mass	Wavelength	Structure
Methylene Blue	$C_{16}H_{18}N_3SCl$	319.9g/mol	660nm	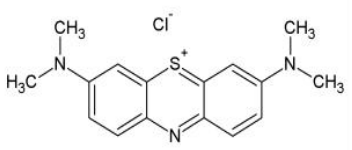

$$NP + h\upsilon \longrightarrow e^- + h^+$$
$$h^+ + H_2O \longrightarrow HO^{\cdot} + h^+$$
$$h^+ + OH^- \longrightarrow OH^{\cdot}$$
$$e^- + O_2 \longrightarrow O_2^{\cdot-}$$
$$O_2^{\cdot-} + H_2O_2 \longrightarrow HO^{\cdot}_2 + OH^-$$
$$HO^{\cdot}_2 + H_2O \longrightarrow OH^- + H_2O$$
$$H_2O_2 \longrightarrow 2\,OH^{\cdot}$$
$$OH^{\cdot} + MB \longrightarrow \text{Intermediate products}$$
$$O_2^{\cdot-} + MB \longrightarrow \text{Degradation products}$$
$$\longrightarrow CO_2, H_2O, NH_3 \text{ and Simple Inorganic salts}$$

Scheme-2: Free Radical Species Generation during the Photodegradation of Methylene Blue [MB] Dye

Table-2: Effect of different Concentrations of MB Dye on the Rate of Degradation under UV Light

10^{-5} [MB]	k 10^{-3} sec^{-1}	Degradation Duration in minutes	Chemical Oxygen demand values (mg L^{-1})	
			Initial Degradation	Final Degradation
1.0	7.7	50	416	16
2.0	9.0	80	592	32
3.0	9.6	100	848	16
4.0	12.7	130	1040	24

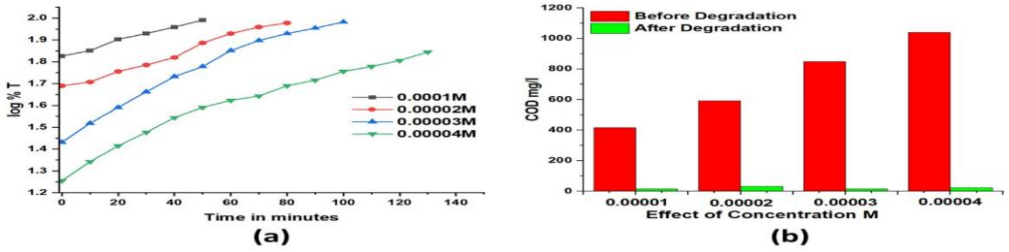

Fig.-7: (a) Effect of Methylene Blue Concentration on Degradation Rate Under UV Light, (b) COD Values

Effect of Catalyst Loading

In order to investigate the impact of catalyst loading, four distinct catalyst dosages ranging from 0.005g, 0.01g, 0.02g, and 0.03g were used, with the dye concentration remaining constant. As seen in Fig.-8(a), the study's findings showed that the Methylene Blue dye solution's degradation efficiency rise as the catalyst's weight grew from 0.005 g to 0.03 g. Furthermore, the photocatalytic activity of the catalyst declines as the catalyst weight is increased above 0.03 g. This is because the NiS/ZrS_2 nanoparticles agglomerate at increasing concentrations, this reduces the availability of active sites on the catalyst and promotes light scattering. Less light tends to flow through the sample as a result. The current study found that 0.03g/20 mL-1 photocatalyst loading is economically optimal. Table-3 and Fig.-8 (b) demonstrate degradation rate constants for different catalyst concentrations and COD values.

Table-3: Effect of Catalyst Loading on Rate of Photodegradation Under UV Light

Catalyst in grams	k 10^{-3} (sec^{-1})	Degradation duration in minutes	Chemical Oxygen demand values (mg L^{-1})	
			Initial Degradation	Final Degradation
0.005	3.4	130	848	16
0.01	8.3	130	848	32
0.02	12.7	100	848	16
0.03	5.5	130	848	48

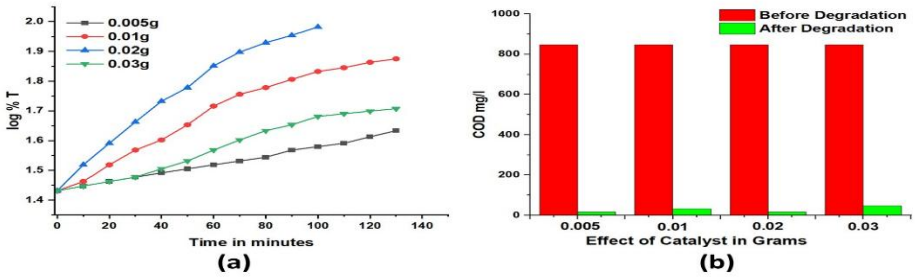

Fig.-8: (a) Effect of Catalyst Loading on Degradation Rate of MB Dye Solution Exposed to UV Light, and (b) COD Results

Effect of pH

When assessing the photodegradation reaction in an aqueous medium, one of the key variables to consider is the pH of solution. The influence of pH was studied at values of 4.0, 6.5, and 8.0, while keeping all other parameters unchanged. Results indicate a consistent increase in photodegradation efficiency across this range, with the highest rate observed at pH 8.0. Consequently, a pH of 8.0 was selected as optimal due to its higher degradation performance. Corresponding rate constants and COD values for this pH dependency are presented in Table-4 and Fig.-9(a) and 9(b)

Table-4: Effect of pH on Photodegradation of Methylene Blue Dye under UV Light

pH	k 10^{-3} (sec^{-1})	Degradation duration in minutes	Chemical Oxygen demand values (mg L^{-1})	
			Initial Degradation	Final Degradation
4.0	5.5	100	848	32
6.5	7.9	100	848	24
8.0	12.7	100	848	16

Temperature Effect

One of the key elements influencing the rate of photodegradation is temperature. The impact of temperature on the degradation of Methylene Blue dye was investigated. The findings demonstrate that degradation efficiency improves at elevated temperatures, with an initially modest reaction rate at lower temperatures. The process becomes considerably more effective at higher temperatures, primarily due to

an increase in the diffusion rate. This acceleration confirms that raised temperatures enhance the overall degradation kinetics[23]. The specific parameters used in this experiment are provided in Table-3. Corresponding rate constants and COD values related to the temperature effect are detailed in Table-5 and illustrated in Fig.- 10(a) and 10(b). Table-6 indicates the thermodynamic parameters at the three different temperatures.

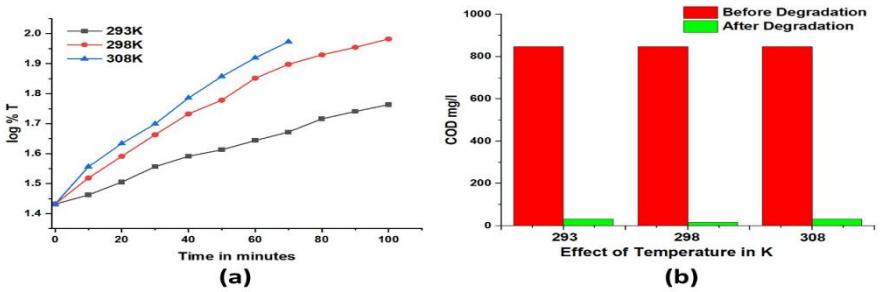

Fig.-9: (a) Effect of pH Degradation Rate of MB Dye Solution and (b) COD Values

Table-5: Effect of Temperature on the Rate of Photodegradation of Methylene Blue Dye under UV Light

Temperature in K	k 10^{-3} (sec^{-1})	Degradation duration in minutes	Chemical Oxygen demand values (mg L^{-1})	
			Initial Degradation	Final Degradation
293	7.7	100	848	32
298	12.6	100	848	16
308	17.4	70	848	32

Table-6: Thermodynamic Parameters for the Photodegradation of Methylene Blue Dye Solution

Temperature (K)	Activation Enthalpy ($\Delta H^{\#}$)(kJ mol^{-1})	Activation Entropy ($\Delta S^{\#}$)(kJ mol^{-1})	Activation free energy ($\Delta G^{\#}$)(kJ mol^{-1})	Energy of activation (E_a)(kJ mol^{-1})
293	21.59	-211.51	83.56	
298	21.55	-208.97	83.82	24.03
308	21.47	-209.14	85.87	

Antibacterial Activity

The antibiotic to be tested for effectiveness is loaded into a nutrient agar medium well. The antibiotic diffuses into the medium, and if the antibiotic or antibiotic drug kills or inhibits the microorganism, no growth will occur in the well's immediate vicinity, which is known as the zone of inhibition. The inhibition zone created around the well and the drug's effect are related. *Staphylococcus aureus* (MTCC 96), *Lactobacillus acidophilus* (MTCC 447), and *Bacillus subtilis* (MTCC 443) were the test bacterial strains that were acquired from MTCC, IMTECH, Chandigarh, India. Measurements of the antibacterial activity" were made using well diffusion techniques. An approximately 25mL volume of melted Mueller-Hinton agar (Himedia, Mumbai, India) was placed in a sterile Petri plate. Plates were grown for eighteen hours after solidification (with the OD set to 0.6). A sterile L-rod spreader was used to evenly distribute 100 µL of the prepared bacterial suspension, creating a uniform lawn culture on the agar plate. A 6-mm well was made on the agar using a sterilised cork-borer after the microorganisms had been incubated for five minutes. The test samples were placed into the wells at 50 µg/well, 100 µg/well, 150µg/well, and 200µg/well concentrations. As a positive control, 30 µg/ml of *azithromycin* was employed. At 37°C, the plates had been incubated for 24 hours in a bacteriological "incubator. Antibacterial activity was measured by measuring the well's zone of inhibition width employing the antibiotic zone scale (Himedia, Mumbai, India).[24–25] As can be seen from the zone of inhibition displayed in Fig.-10 and 11, and Table-7, the test samples demonstrated strong antibacterial activity against the test bacterial strains *Bacillus subtilis* (MTCC 443), *Lactobacillus acidophilus* (MTCC 447), and *Staphylococcus aureus* (MTCC 96").

Table-7: Antibacterial Activity of NiS/ZrS_2 Nanoparticles Against Different Strains of Bacteria

Sample name	Zone of inhibition (millimeter)					Zone of inhibition Standard (millimeter)
	0 (µg/ml)	50 (µg/ml)	100 (µg/ml)	150 (µg/ml)	200 (µg/ml)	30 µg/well
Bacillus subtilis	-	17	22	24	26	22
Lactobacillus acidophilus	-	14	18	20	24	17
Staphylococcus aureus	-	12	14	17	18	20

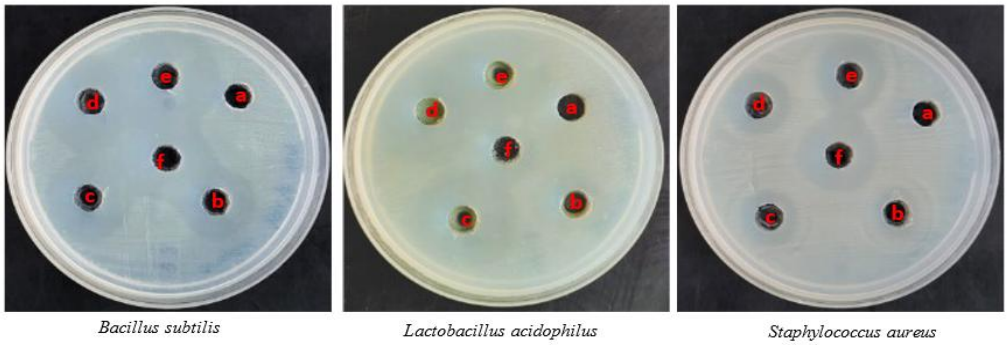

Fig.-10: Antibacterial Activity of Test Sample: a. 0 µg/mL, b. 50 µg/mL, c. 100 µg/mL, d. 150µg/mL, e. 200µg/mL, f. *Azithromycin* (30µg/mL)

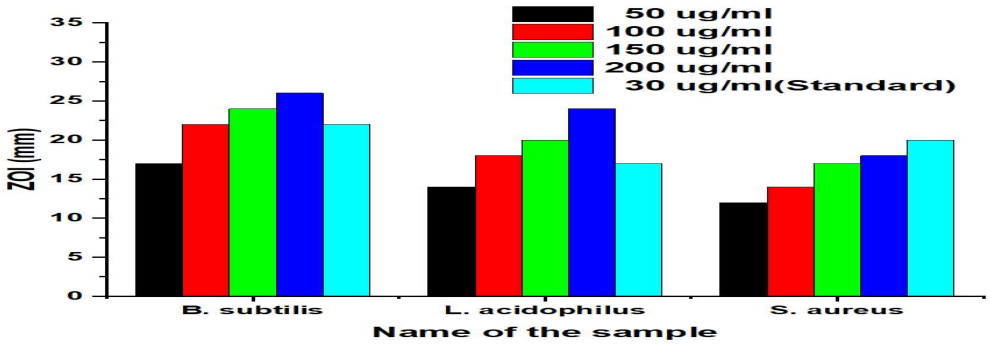

Fig.-11: Antibacterial Activity- Comparison Chart

CONCLUSION

This study presents the synthesis of NiS/ZrS_2 nanoparticles using a novel, cost-effective, and environmentally benign electrochemical method. The photodegradation of these semiconductors offers an eco-friendly way to remove dangerous materials from industrial effluents and wastewater. The dynamics of methylene blue degradation have been studied. According to the kinetics of Methylene Blue dye photodegradation, first-order kinetics should be followed while demineralising the dye. The complete degrading response was verified using the COD experiment. The produced nanoparticles' biological activity as potent antimitotic and antibacterial agents is supported by their ability to limit cell growth by penetrating *Bacillus subtilis*, *Lactobacillus acidophilus*, and *Staphylococcus aureus* cells. When Ni and Zr are present, the rate of photo-catalytic activity is inhibited. UV radiation blocking and cosmetics preparation are possible with the NiS/ZrS_2 nanocomposite.

ACKNOWLEDGEMENTS

The authors express their sincere gratitude to the late Professor S. Ananda, former Professor and Chairman, UGC–BSR Faculty Fellow, Department of Studies in Chemistry, Manasagangothri, University of Mysore, Mysuru, for his invaluable guidance and encouragement throughout this work. Appreciation is also extended to Yuvaraja's College and the support provided under the IOE, UPE, and CPEPA programs of the University of Mysore.

CONFLICT OF INTERESTS

The authors declare that there is no conflict of interest.

AUTHOR CONTRIBUTIONS

The present work is related to *SDG-6: Clean Water and Sanitation*. It's Closest for research on water purification and wastewater treatment. All the authors contributed significantly to this manuscript, participated in reviewing/editing and approved the final draft for publication. The research profile of the authors can be verified from their ORCID ids, given below:

H. S. Sindhushree https://orcid.org/0009-0000-9459-8370
R. T. Radhika https://orcid.org/0009-0001-6884-8521
B. M. Venkatesha https://orcid.org/0009-0001-7332-2591

Cite this article as: H. S. Sindhushree *et al.*, *Rasayan J. Chem.*, 19(2), 1069-1078(2026), https://doi.org/10.317 88/RJC.2026.1929560.

REFERENCES

1. H.R. Rajabi and M. Farsi, *Materials Science in Semiconductor Processing*, **31**, 478(2015), https://doi.org/10.1016/j.mssp.2014.11.044
2. X. Li, H. Xu, Z.S. Chen and G. Chen, *Journal of Nanoamterials*, **Volume 2011**, Article ID 270974(2011), https://doi.org/10.1155/2011/270974
3. U.S. Senapati, D.K. Jha and D. Sarkar, *Research Journal of Physical Sciences*, **1**, 1, (2013),
4. U. Baishya and D. Sarkar, *Indian Journal of Pure and Applied Physics*, **49**, 186(2011).
5. Sohail Saeed and Naghmana Rashid, *Cogent Chemistry*, **1(1)**, Article: 1030195 (2015), https://doi.org/10.1080/23312009.2015.1030195
6. J. Lopez, W.R. Aguirre-Contreras, M.E. Gomez and G. Zambrano, *International Journal of Applied Science and Engineering Technology*, **6**, 47(2017).
7. H.C. Charan Kumar, R. Shilpa and S. Ananda, *Journal of Nanoscience and Technology*, **5(5)**, 840(2019), https://doi.org/10.30799/jnst.278.19050505
8. A.V. Gole and S. Shivram, *Advanced Materials Research*, **383-390**, 3828(2011), https://doi.org/10.4028/www.scientific.net/AMR.383-390.3828
9. Farsi and Mohammad, *Journal of Molecular Catalysis A: Chemical*, **399**, 53(2015), https://doi.org/10.1016/j.molcata.2015.01.029
10. D.T. Hodul, *Journal of Solid State Chemistry*, **62(3)**, 328(1986), https://doi.org/10.1016/0022-4596(86)90247-1
11. D. R. Linde, *CRC Handbook of Chemistry and Physics: A Ready-Reference Book of Chemical and Physical Data,* CRC Press, Boca Raton, FL, (2008).
12. D. R. Lide. Zirconium. In *CRC Handbook of Chemistry and Physics* (88th ed.), CRC Press, (2007-2008).
13. L. Perk. The Future of Immune-PET in Drug Development: Zirconium-89 and Iodine-124 as Key Factors in Molecular Imaging , *Doctoral dissertation*, VU University Amsterdam, 2009.
14. J. R. Ingelfinger, *The New England Journal of Medicine*, **372(3)**, 2015, https://doi.org/10.1056/NEJMe1414112

15. J. Pelleg, E. Elish and D. Mogilyanski, *Metallurgical and Materials Transactions A*, **36**, 3187(2005), https://doi.org/10.1007/s11661-005-0089-0
16. J. Abdul Nasir, M. Hafeez, M. Arshad, N.Z. Ali, I.F. Teixeira, I. McPherson, Zia-ur-Rehman and A. Khan, *ChemSusChem*, **11(15)**, 2587(2018), https://doi.org/10.1002/cssc.201800583
17. A.A. Peter and E.O. Abimbola, *Nanomaterials,* **11**, 8,(2021), https://doi.org/10.3390/nano11081990
18. H.C. Charan Kumar, R. Shilpa and S. Ananda, *Journal of Applicable Chemistry*, **9**, 1, (2020)
19. Mi. L. Chen, Y. Wei, W. Chen, W. Hou, and H. Zheng, *Royal Society of Chemistry Advances*, **3**, 18320(2013), https://doi.org/10.1039/C3RA42490A
20. T. A. Geleta and T. Imae, *Bulletin of the Chemical Society of Japan*, **93(4)**, 611(2020), https://doi.org/10.1246/bcsj.20200001
21. Rakesh, S. Ananda, N. M. Gowda and K. R. Raksha, *Advances in Nanoparticles*, **3(4)**,133 (2014), https://doi.org/10.4236/anp.2014.34018
22. K. Cruz-Rodriguez, R. García-Alamilla, C. E. Ramos-Galván, F. Paraguay-Delgado, R Silva-Rodrigo, B. E. Handy and S. Robles-Andrade, *Reaction Kinetics, Mechanisms and Catalysis*, **120**, 279(2017), https://doi.org/10.1007/s11144-016-1093-7
23. M. A. Rauf, I. Shehadeh, A. Ahmed and A. Al-Zamly, World Academy of Science, Engineering and Technology, **55**, 608(2009).
24. K. R. Raksha and S. Ananda, *Journal of Applicable Chemistry*, **3(1)**, 1(2014), http://dx.doi.org/10.4236/mrc.2017.61003
25. L. Wei, C. Shifu, Z. Wei and Z. Sujuan, *Journal of Hazardous Materials*, **164(1)**, 154(2009), https://doi.org/10.1016/j.jhazmat.2008.07.140
26. I. A. Holder and S. T. Boyce, *Burns*, **20(5)**,426(1994), https://doi.org/10.1016/0305-4179(94)90035-3
27. S. Magaldi, S. Mata-Essayag, C. Hartung de Capriles, C. Perez, M. T. Colella, C. Olaizola, and Y. Ontiveros, *International Journal of Infectious Diseases*, **8(1)**, 39(2004), https://doi.org/10.1016/j.ijid.2003.03.002

[RJC-9560/2025]